

FFYS7086 Signal and Image Processing course

PET Modeling

13:15-14:00, 2022.05.11

Hidehiro Iida

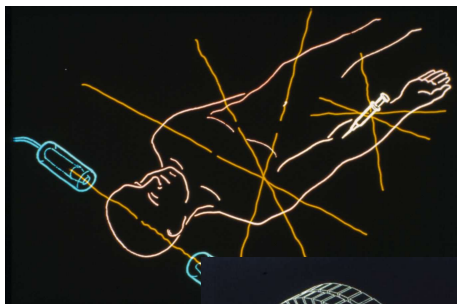
Turku PET Centre

University of Turku Faculty of Medicine

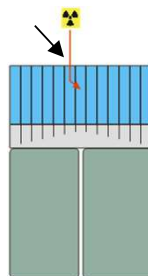
Finland

Positron Emission Tomography

Detector+electronics technology



PET system



- Block design (high packing rate)
- Energy resolution
- Time resolution
- Increased signals
- Electronics circuit (ASIC)
- Large scale storage

$10^4 \sim 10^5$ detectors $\sim 10^9$ の LOR

Coincidence $\Delta t \sim \text{nsec}$

$\sim 200\text{ps}$ for time-of-flight reso.

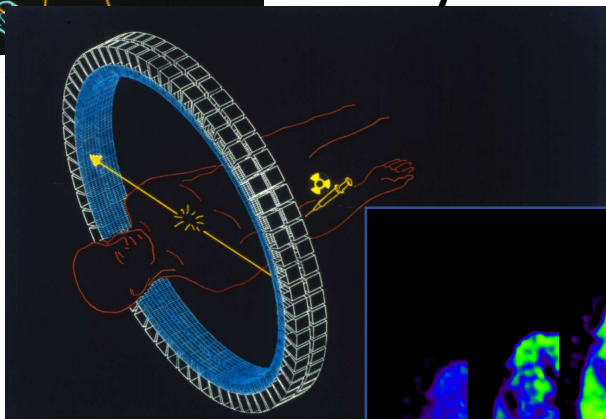
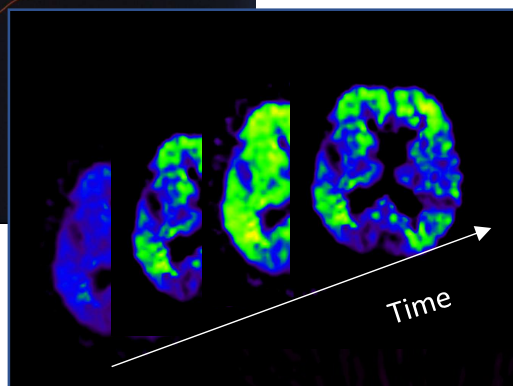


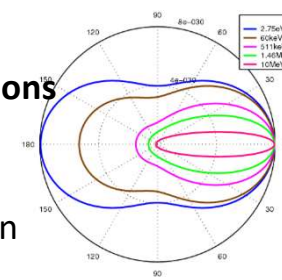
Image reconstruction



Time

A number of corrections

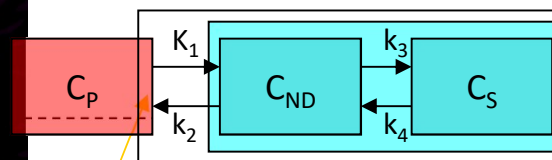
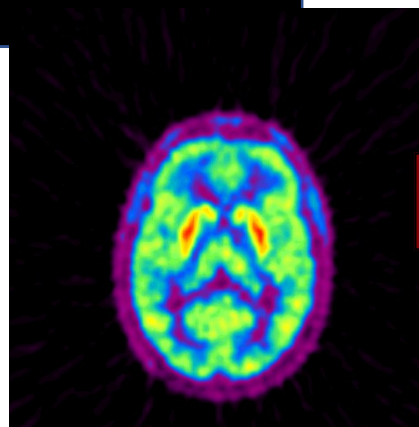
- Random events
- Inhomogeneity
- Dead time
- Photon Attenuation
- Photon Scatter
- Partial Volume



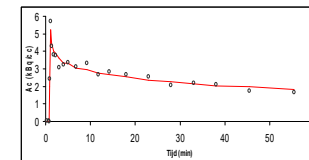
Modeling contribute:

- Practical protocol design
- Radio-tracers development
- PET system design specifications
- Software specifications

To extract biological information



V_B



PET Modeling

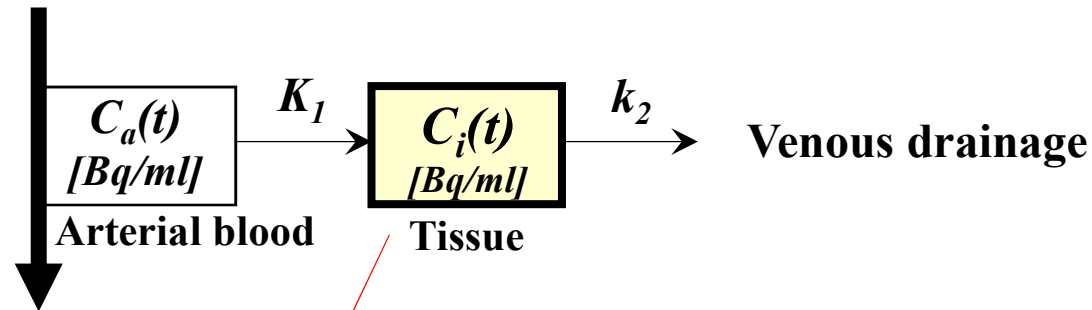
13:15-14:00, 2022.05.11

Contents

- 1. Basis of the compartment model**
- 2. Modeling of H_2^{15}O -based regional tissue perfusion**
 - Cerebral blood flow (CBF)
 - Myocardium blood flow (MBF)
- 3. General concerns and future perspectives**

Exponential function as the basis of the compartmental modeling

Arterial blood supply

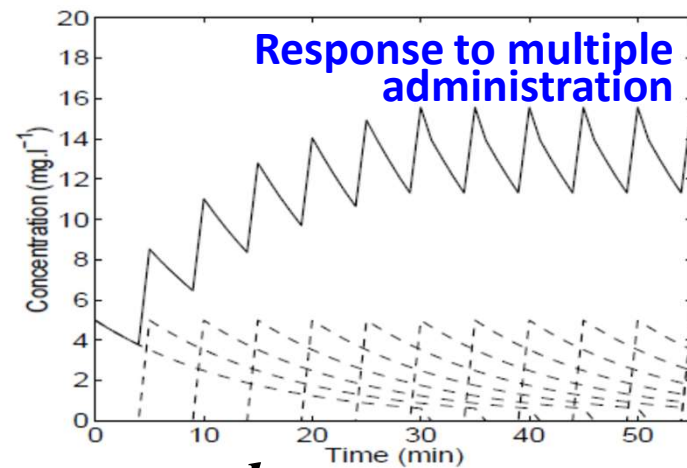
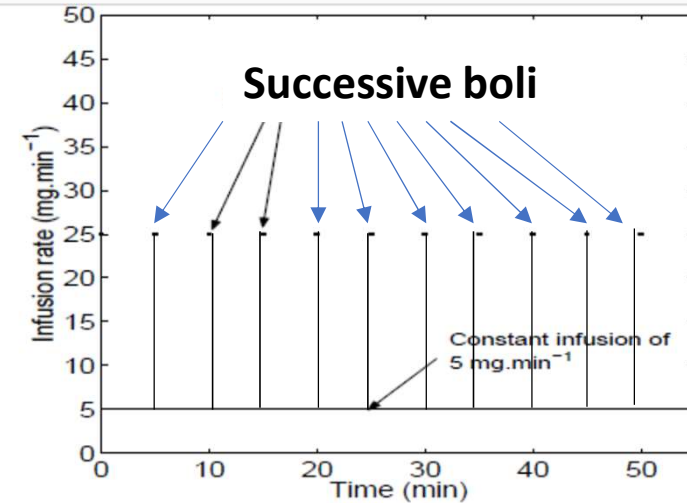
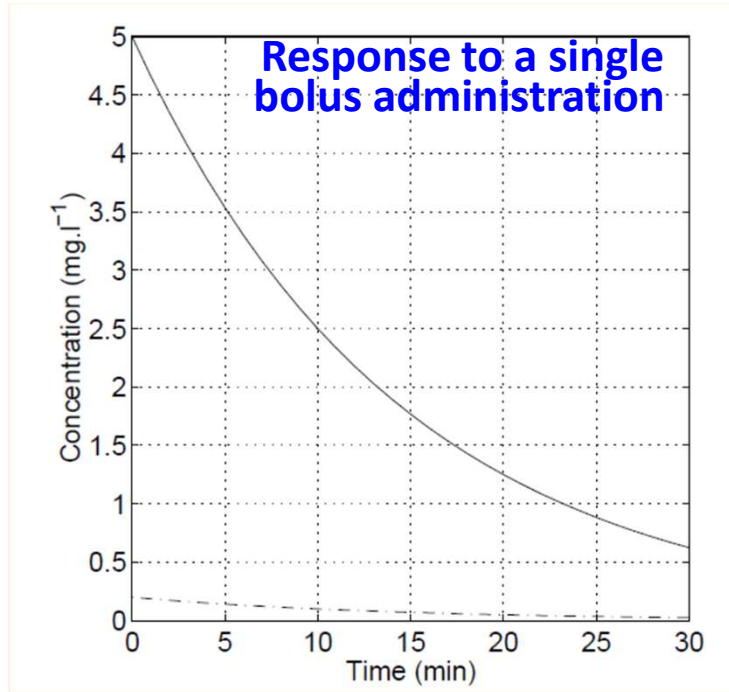


$$\frac{dC_i(t)}{dt} = K_1 C_a(t) - k_2 C_i(t) \quad - \text{eq. (1)}$$

- After the tracer is introduced, the radio-labeled tracer in the arterial blood is carried to tissue, and from the tissue to the venous drainage.
- These transport flux is proportional to differences in concentrations at the boundary, where the carriage rate may be assumed at constant, under some circumstances. Instantaneous equilibrium in the tissue compartment is also an important assumption.
- The time balance of the tracer concentration in the tissue compartment may be expressed as eq. (1).

Solving the compartment model

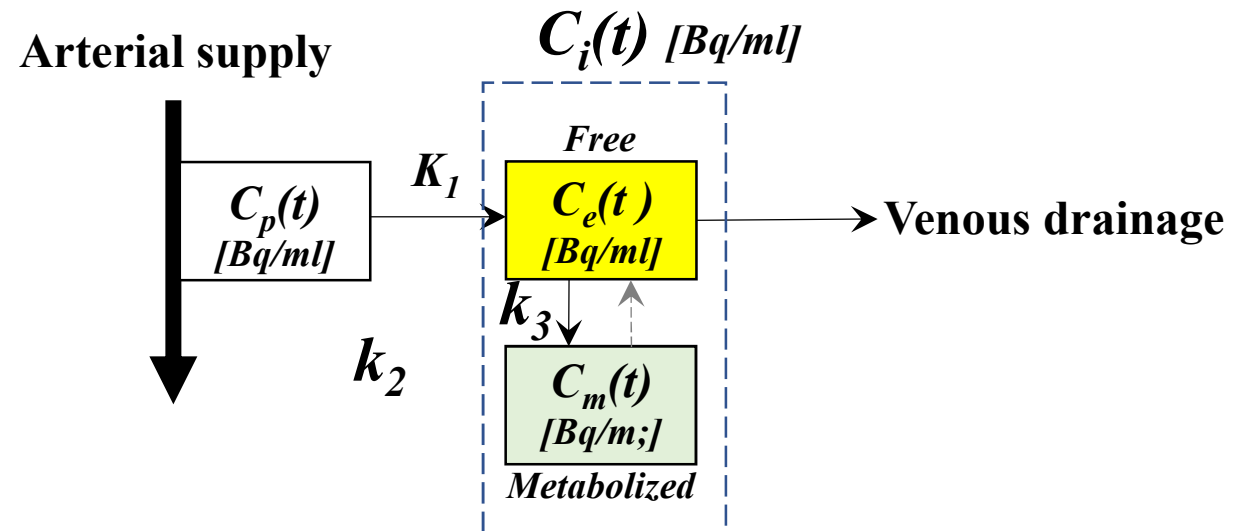
$$\frac{dC_i(t)}{dt} = K_1 C_a(t) - k_2 C_i(t)$$



$$C_i(t) = K_1 \cdot C_a(t) \otimes e^{-\frac{k_2 \cdot t}{p}}$$

$$= K_1 \cdot \int_0^t C_a(t-s) \cdot e^{-\frac{k_2 \cdot s}{p}} ds$$

Exponential function as the basis of the compartmental modeling



$$\bullet \frac{dC_e(t)}{dt} = K_1 C_p(t) - k_2 C_e(t) - k_3 C_e(t)$$

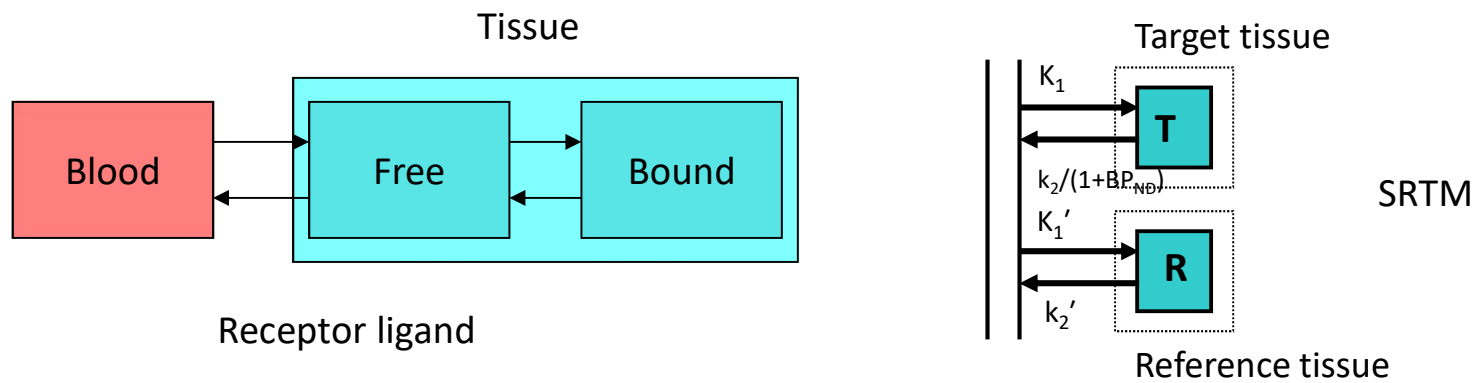
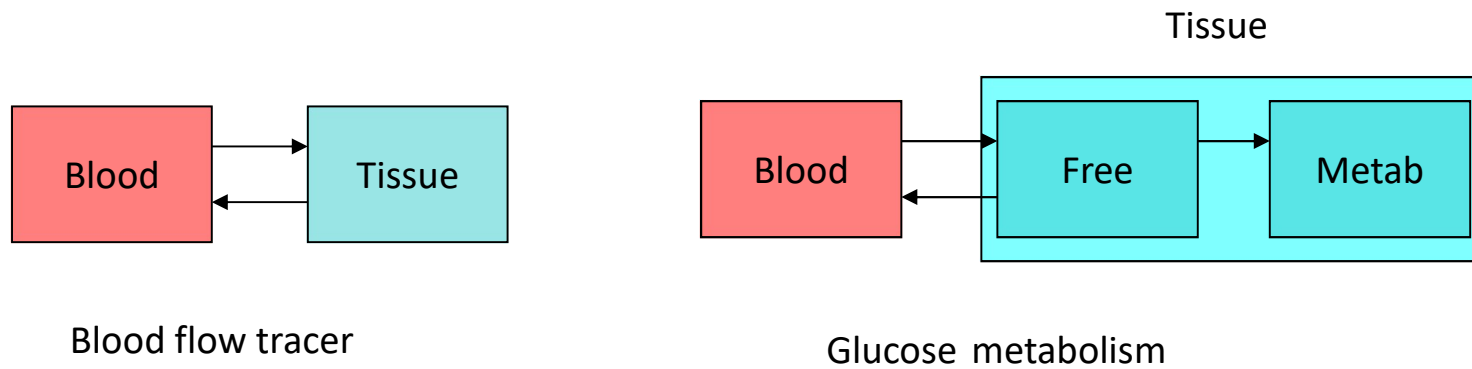
$$\bullet \frac{dC_m(t)}{dt} = k_3 C_e(t)$$

$$C_i(t) = C_e(t) + C_m(t)$$

$$= \frac{K_1}{(\alpha_2 - \alpha_1)} \underbrace{\{(k_3 - \alpha_1)e^{-\alpha_1 \cdot t} + (\alpha_2 - k_3)e^{-\alpha_2 \cdot t}\}}_{C_e(t)} + \frac{K_1 k_3}{(\alpha_2 - \alpha_1)} \underbrace{(e^{-\alpha_1 \cdot t} - e^{-\alpha_2 \cdot t})}_{C_m(t)} \otimes C_p(t)$$

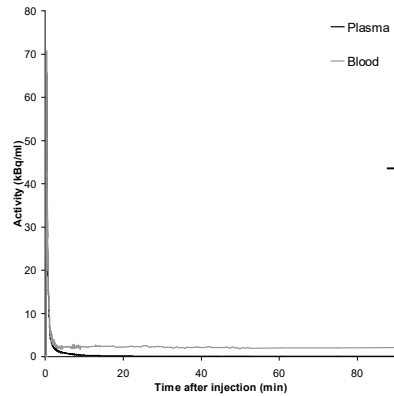
$$\alpha_{1,2} = \frac{1}{2} \cdot \left[(k_2 + k_3 + k_4) \mp \sqrt{(k_2 + k_3 + k_4)^2 - 4k_2 k_4} \right]_p$$

Common Compartment Models

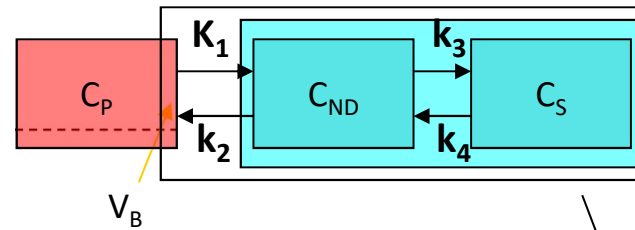


Kinetic fitting to solve the inverse problem

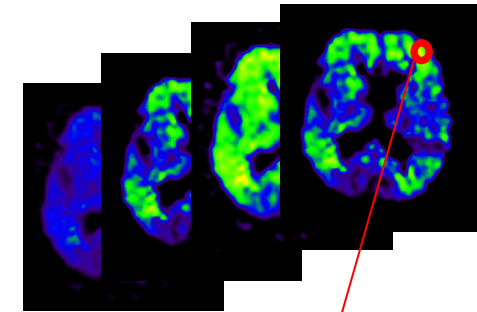
Input function



Kinetic model



Dynamic PET images



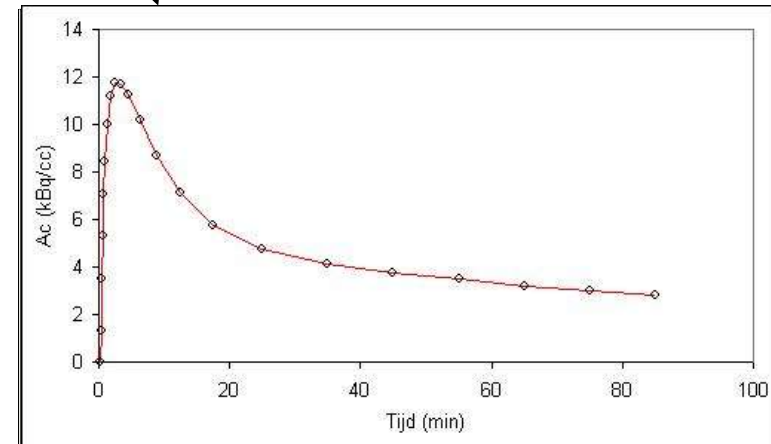
Fitting routine

Tissue time-activity curve

Kinetic parameters

K_1 : transport

K_3/k_4 : binding potential



Optimization of parameter sets (p_1, p_2, p_3, \dots)

Counts $\left[\frac{Bq}{ml}\right]$ estimated using a formulae
with given K_1, k_2, k_3, \dots values

Counts $\left[\frac{Bq}{ml}\right]$ measured by PET

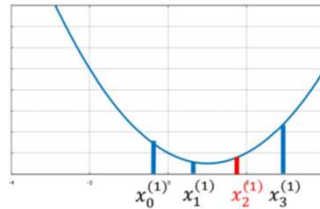
$$\chi^2 = \frac{1}{N} \cdot \sum_i \left(\frac{(\text{Estimated data})_i^2 - (\text{Measured data})_i^2}{(\text{Estimated error})_i^2} \right)$$

If the assumed model formula is adequate, and the data are acquired with sufficient accuracy, the minimal χ^2 value may reach unity.

- “The minimal $\chi^2 \ll 1$ ” means that the parameters determined are not reliable.
- “The minimal $\chi^2 \gg 1$ ” suggests the need for improving the model formulation.

Numerical procedures to find the local minimum of χ^2

➤ 1-dimensional search to find a local minimum

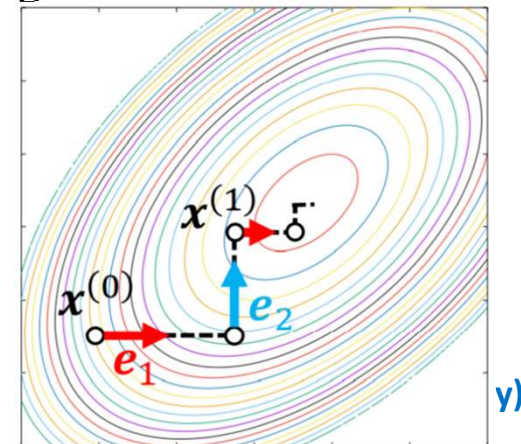


Golden section method, etc
(No way to find the “global” minimum!)

➤ Multi-parameter search

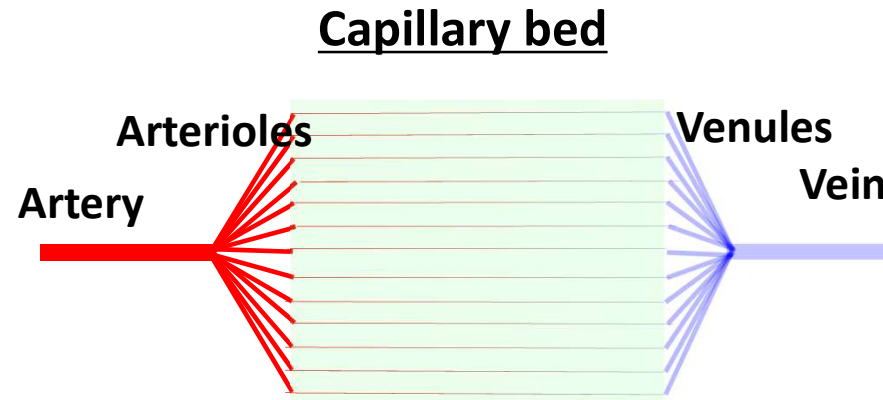
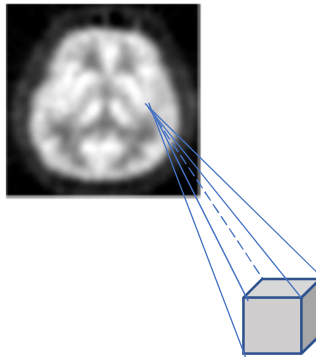
- The steepest descent method
 - Conjugate gradient method
 - Newton's method
 - Gauss-Newton method
 - Marquardt method
 - Powell method, etc.
 - Simplex (Nelder-Mead) method
- Works well!!!

Combination with 1-dimensional search
+ updating the search direction



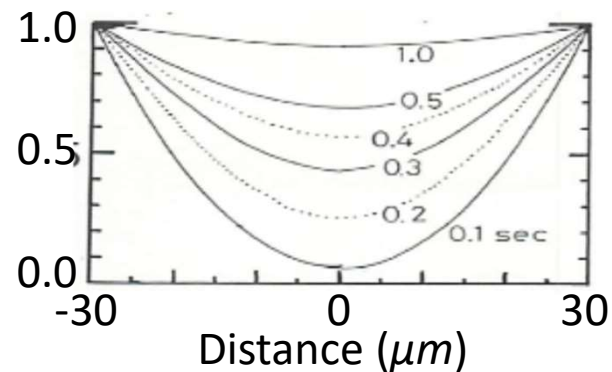
➤ Basis Function method accelerates the optimization

Modeling of ^{15}O -labeled water (H_2^{15}O) kinetics for cerebral & myocardial blood flow

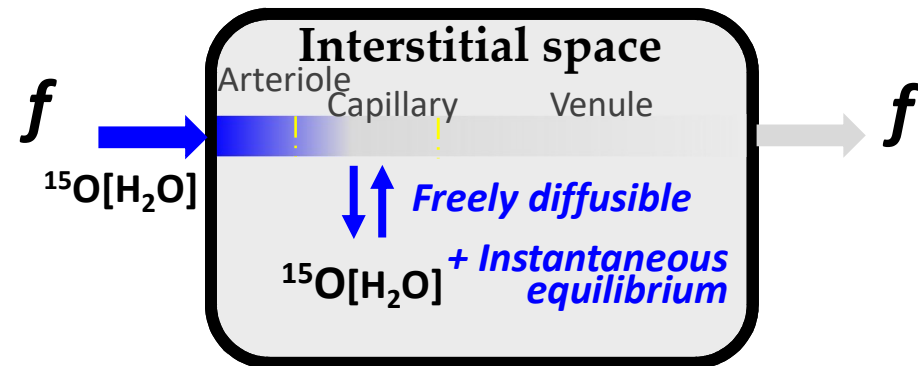


Diffusion equation in the capillary bed

$$\frac{\partial u(t,r)}{\partial t} = D \frac{\partial^2 u(t,r)}{\partial r^2}$$



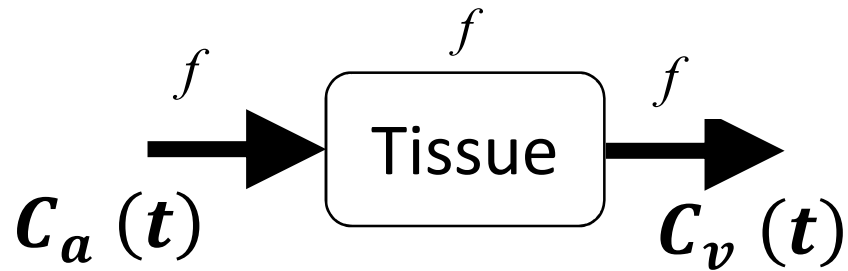
Single-tissue compartment model



Questions and proposals

- Gradient along the capillary
- Slowly exchanging water (binding water)
- Heterogeneity of blood supply

Mathematical model for H_2^{15}O to quantitatively assess regional blood flow



$$\frac{dC_i(t)}{dt} = f \cdot C_a(t) - f \cdot C_v(t)$$

Assuming $C_v(t) = \frac{C_i(t)}{p}$

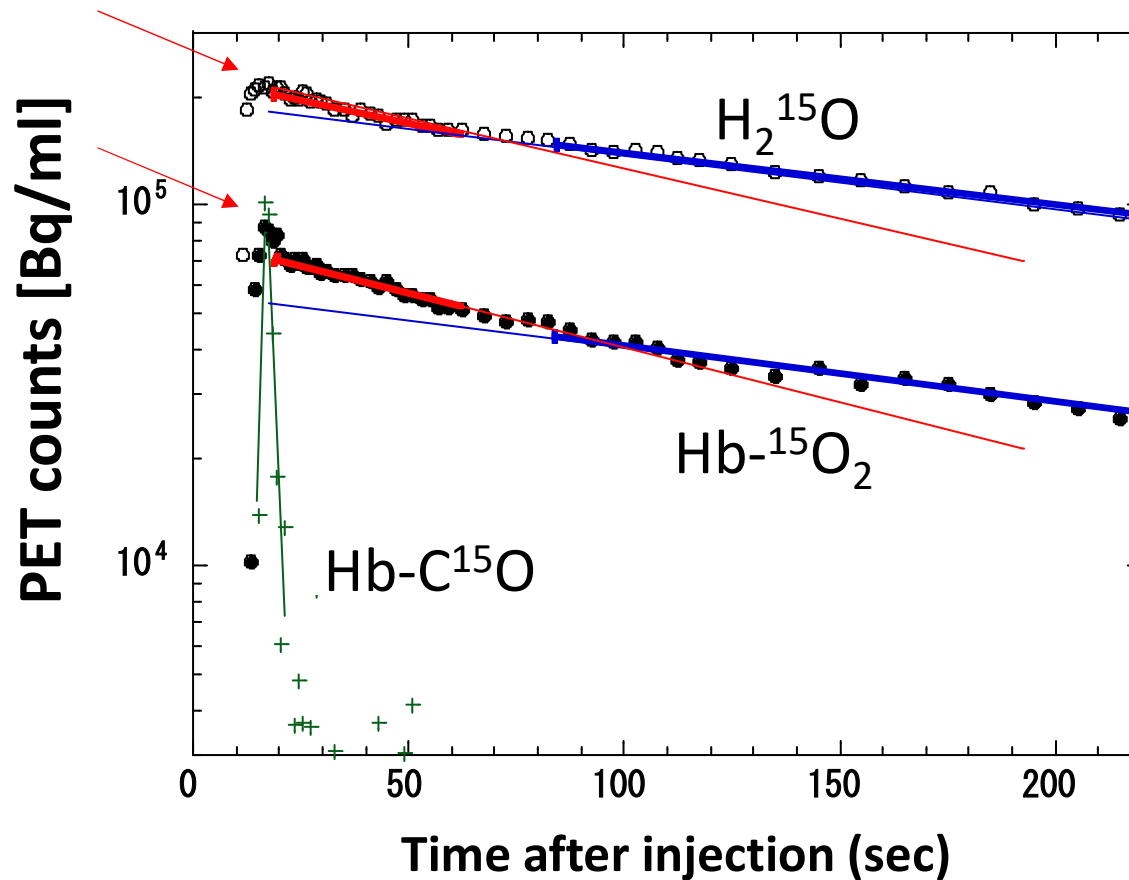
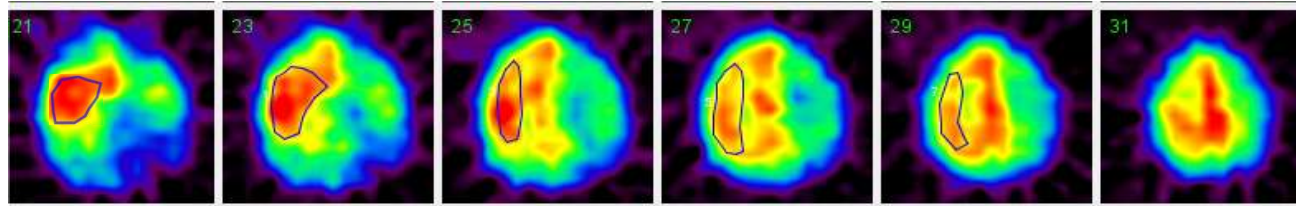
$$\because p = \frac{\text{Water content in tissue}}{\text{Water content in blood}}$$

$$\rightarrow \frac{dC_i(t)}{dt} = f \cdot C_a(t) - f \cdot \frac{C_i(t)}{p}$$

Solving eq. (1) gives

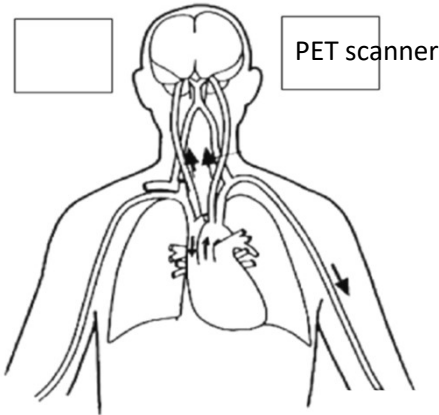
$$C_i(t) = f \cdot C_a(t) \otimes e^{-\frac{f}{p} \cdot t}$$

Clearance of radioactivity from cerebral tissue after bolus carotid injection of ^{15}O -water

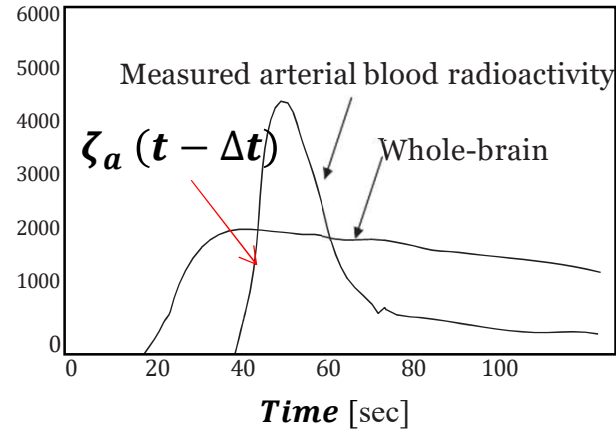


Delay and dispersion in the observed AIF occur in the arterial lines and in the catheter tubes.

A)



C)



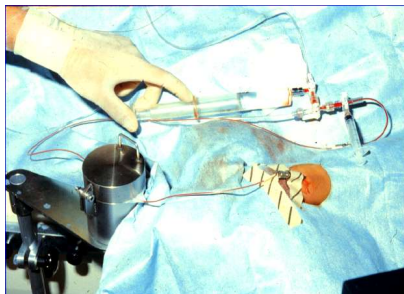
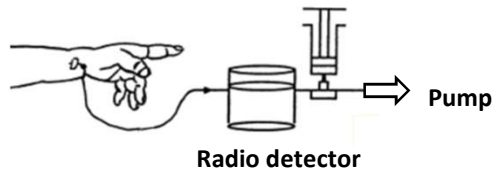
Dispersion function:

$$d(t) = \frac{1}{\tau} \cdot e^{-t/\tau}$$

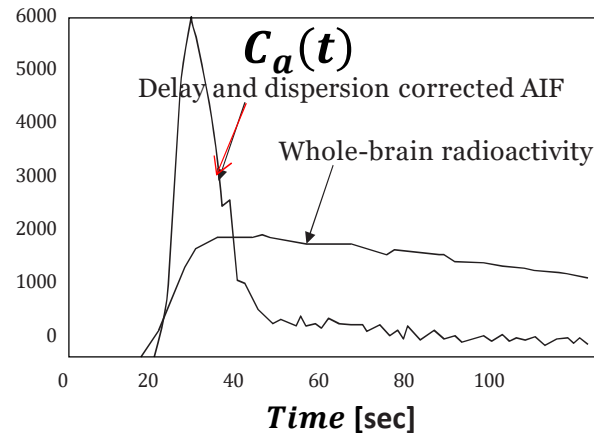
Delayed & Dispersed AIF:

$$\zeta_a(t - \Delta t) = C_a(t) \otimes \frac{1}{\tau} \cdot e^{-t/\tau}$$

B)



D)

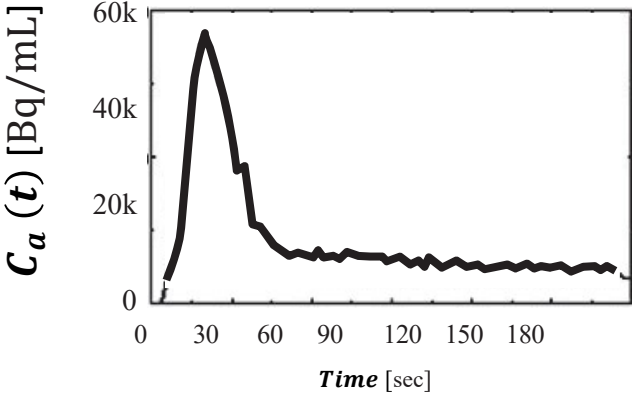


Delay & Dispersion corrected AIF:

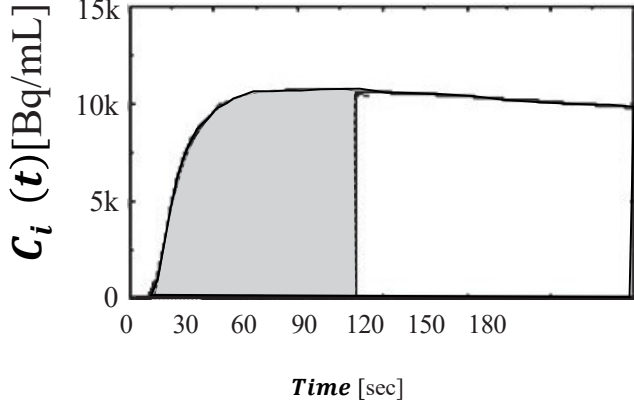
$$C_a(t) = \zeta_a(t - \Delta t) + \tau \frac{d}{dt} (\zeta_a(t - \Delta t))$$

Procedures of the ^{15}O -Water Autoradiography

Arterial input function



Tissue TAC

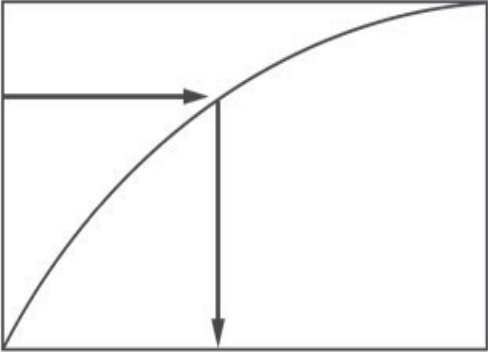


Pixel counts measured by PET

$$\int_0^t C_i(t) dt = f \cdot \int_0^t C_a(t) \otimes e^{-\frac{f}{p}t} dt$$

|
Assumed **p**-value

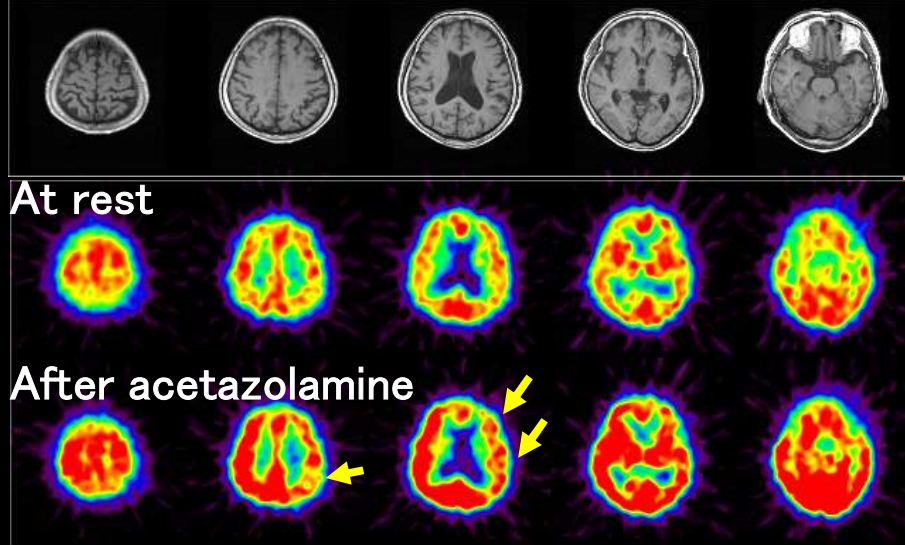
Calculation of CBF by Table-Look-Up



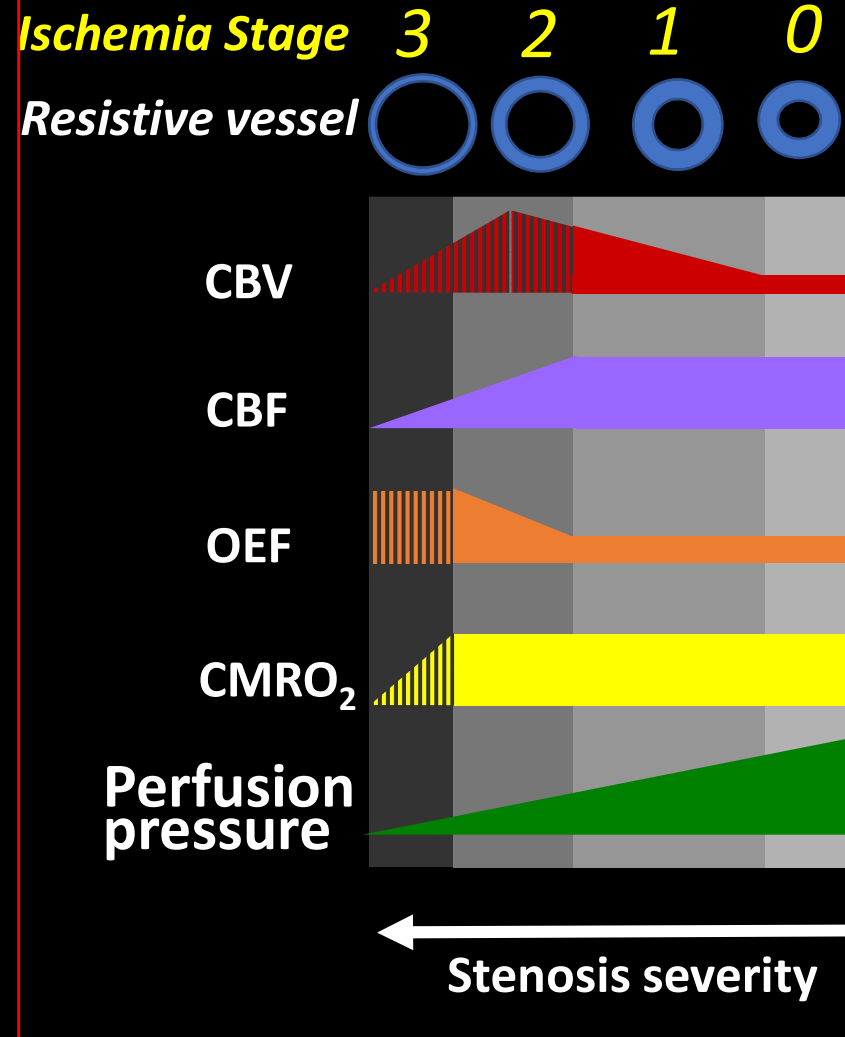
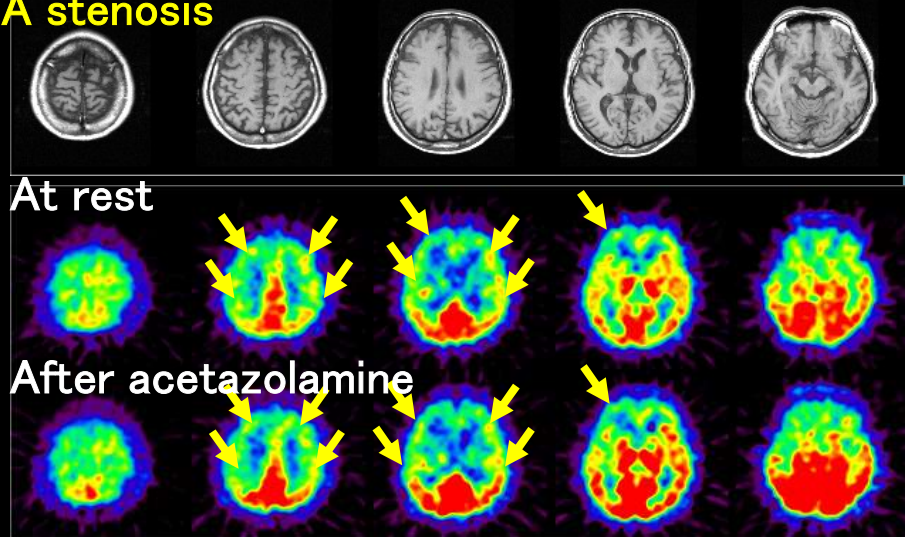
CBF image

CBF images at rest and after ACZ by ^{15}O -Water and PET

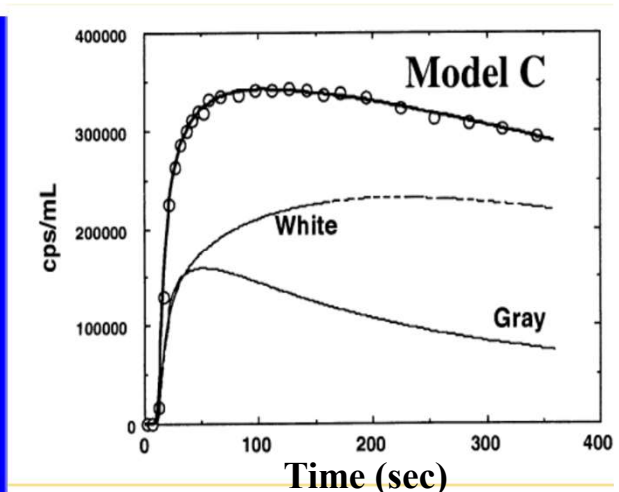
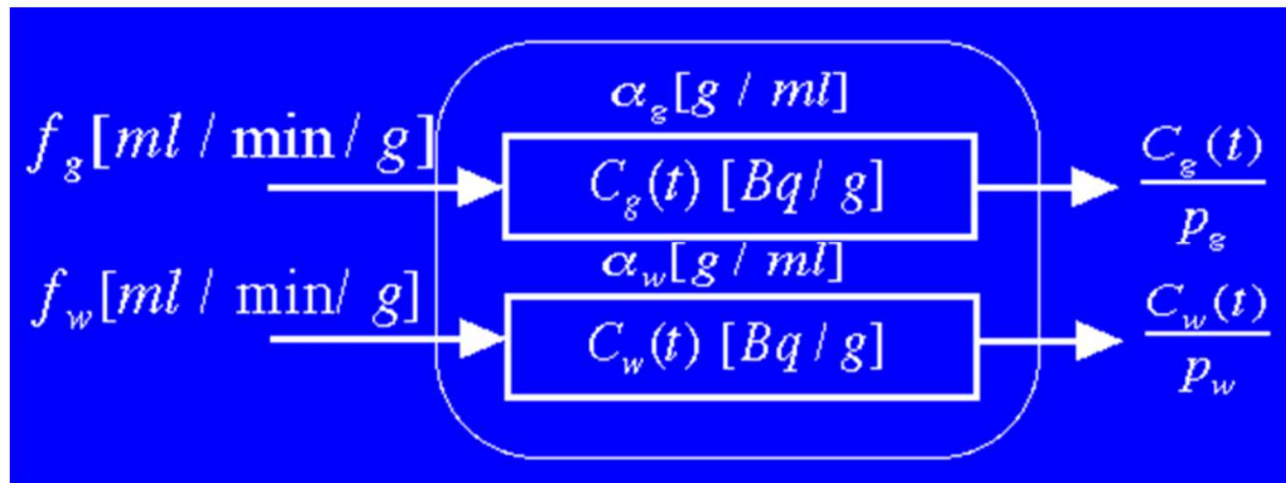
Case 1: Patients with lt ICA stenosis



Case 2: Patients with rt ICA occlusion & lt ICA stenosis



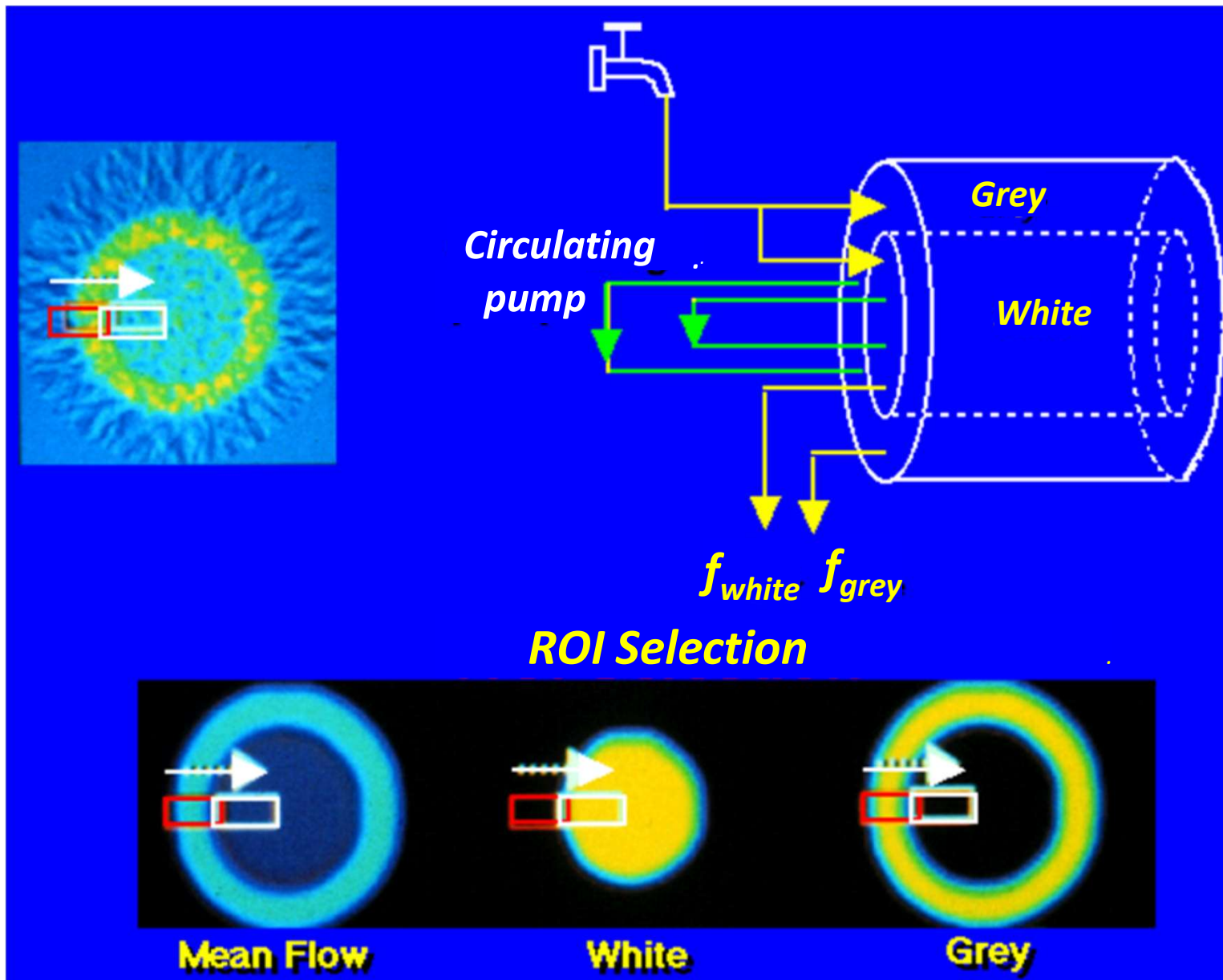
Quantitation of rCBF corrected for Partial Volume Effect using ^{15}O -Water and PET



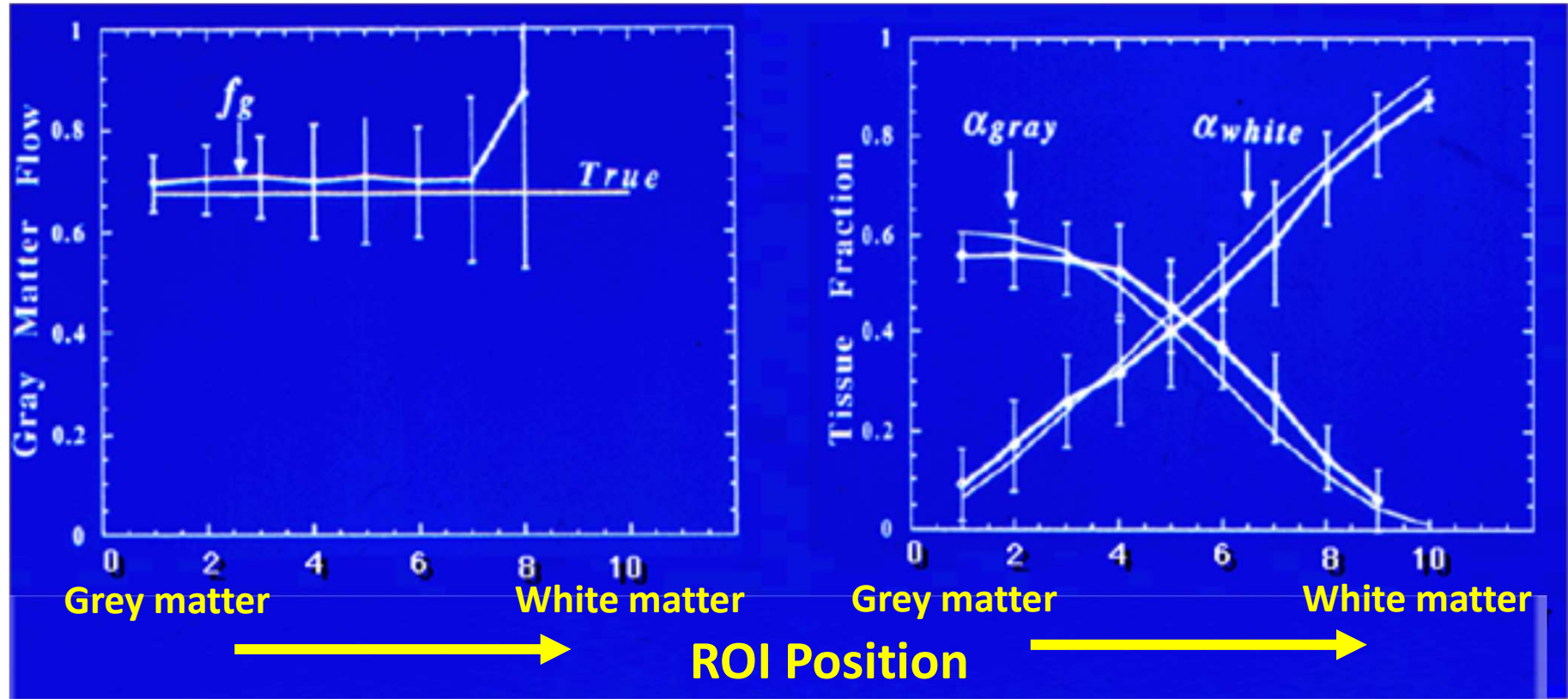
$$R(t) = \alpha_g \cdot f_g \cdot C_a(t) \otimes e^{-\frac{f_g}{p_g} t} + \alpha_w \cdot f_w \cdot C_a(t) \otimes e^{-\frac{f_w}{p_w} t}$$

*Iida H, Law I, etc, JCBFM 2000
Law et al., Iida et al. JCBFM 2000*

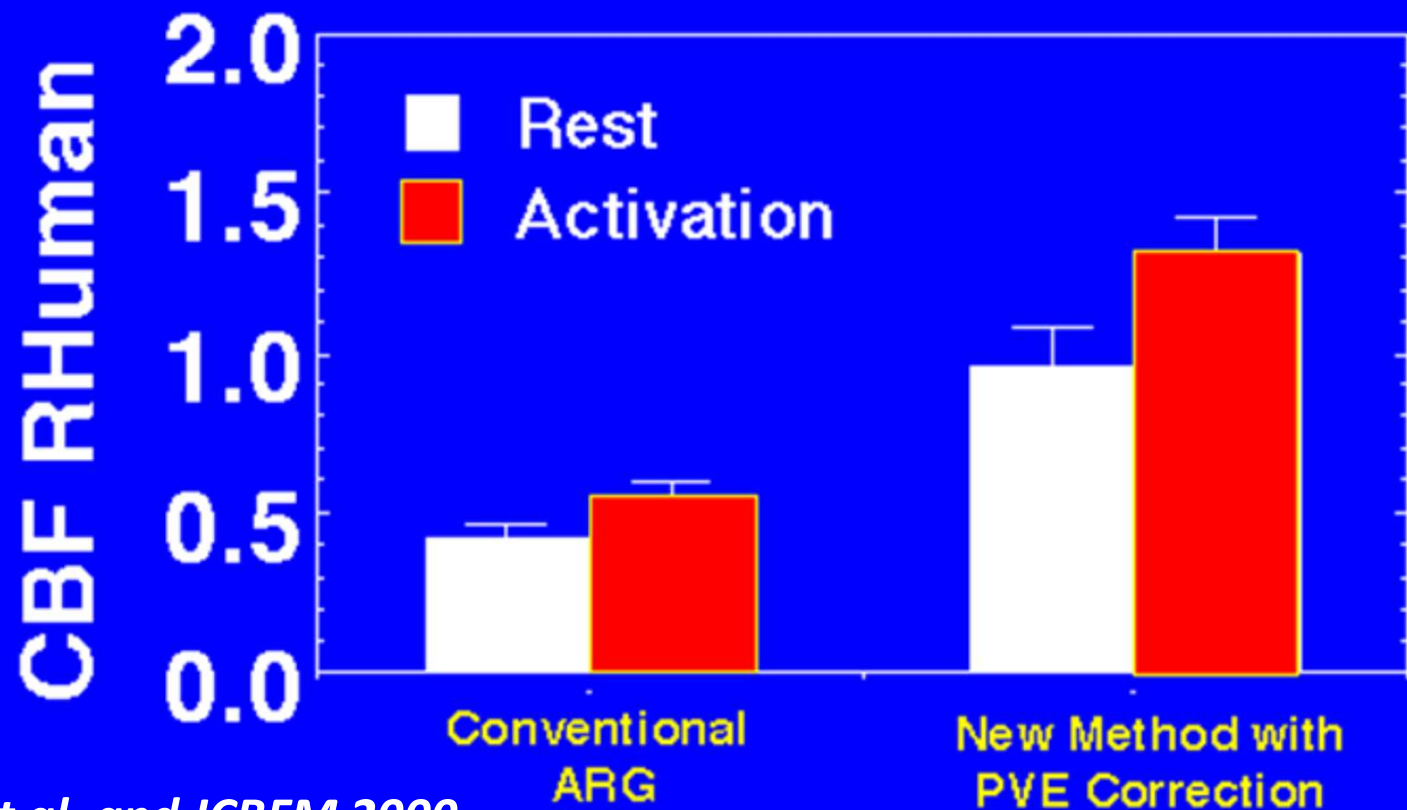
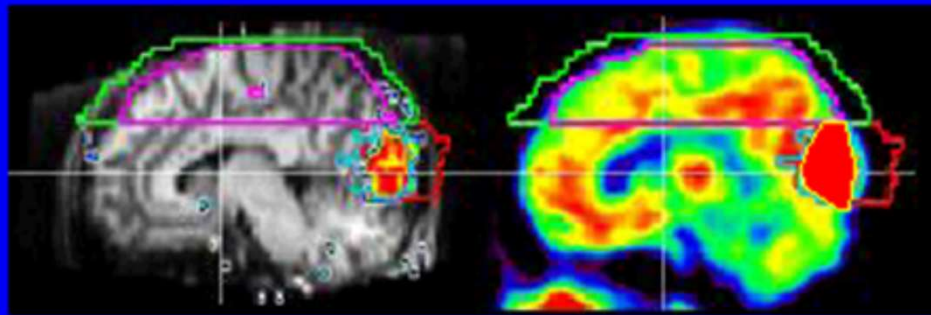
Validation using a dynamic equilibrium phantom



Results from a dynamic equilibrium phantom experiment

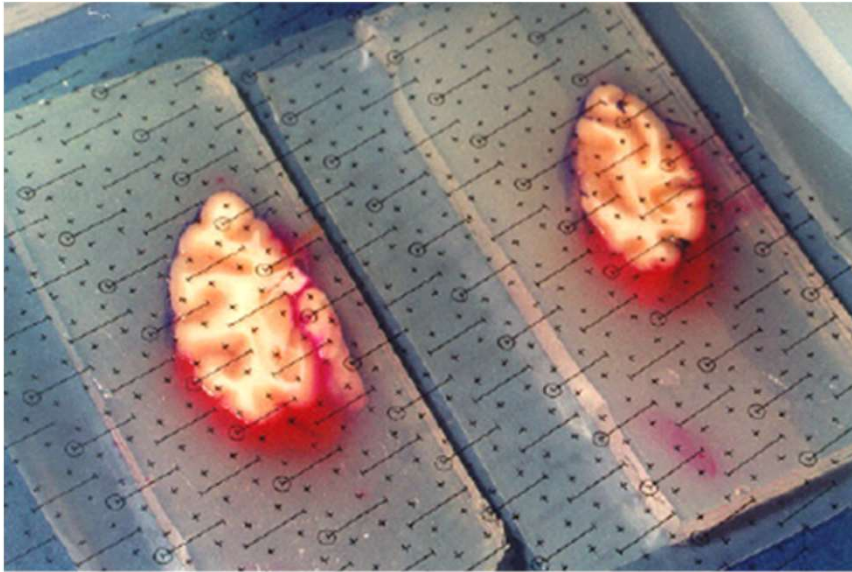


Impact of Partial Volume Correction on Absolute CBF in young healthy volunteers



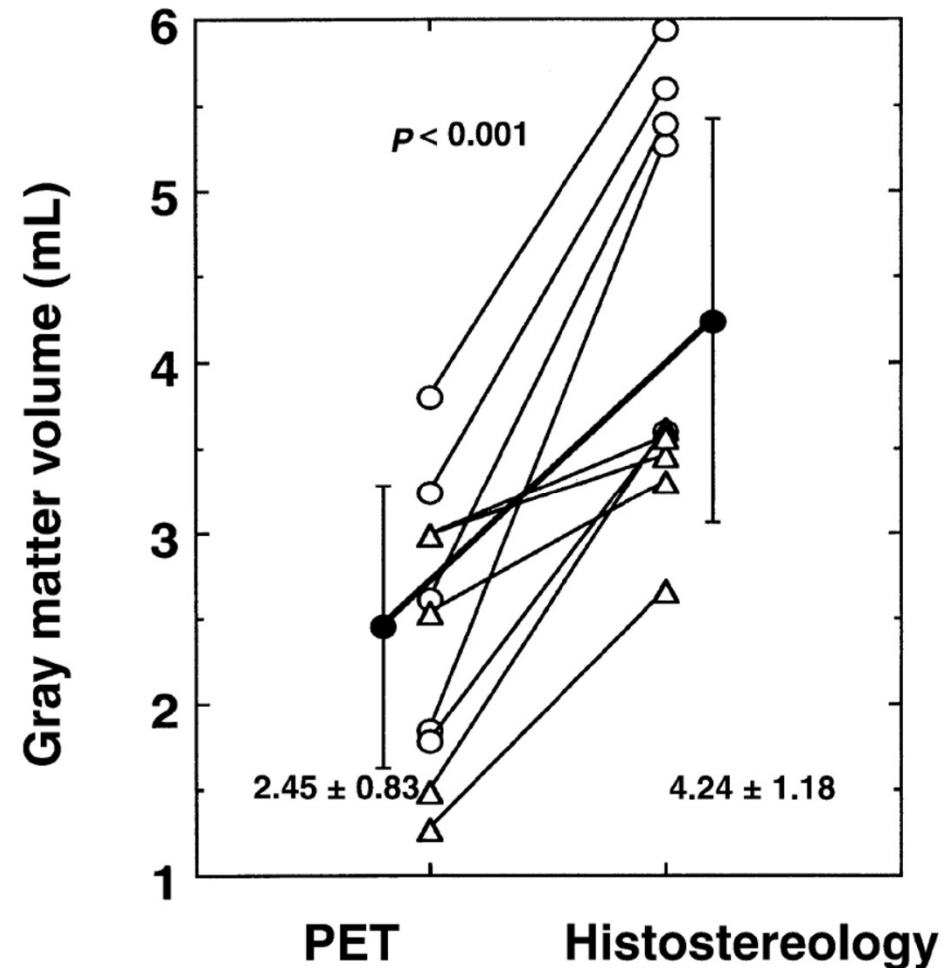
Law I et al. and Iida et al. and JCBFM 2000

Comparison of the gray matter volumes - ^{15}O -water PET vs stereologic volumes -



$$V = \bar{t} \times a(p) \times \sum p$$

\bar{t} = average section thickness
 $a(p)$ = areaper point of the grid
 $\sum p$ = the total number of points that fall on the object



lida et al. abd Law I et al., JCBFM 2000

Quantitation of myocardial perfusion

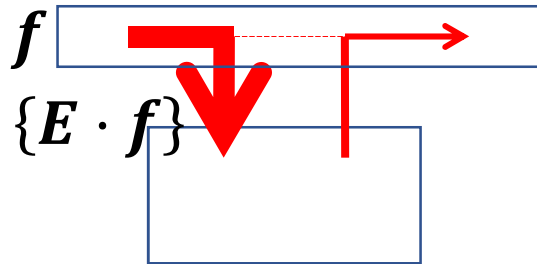
¹⁵O-water as a gold standard

- 1. Instantaneous equilibrium in tissue**
- 2. Large first-pass extraction fraction**
- 3. Chemically inert**
 - No retention
 - No metabolism
 - Adequate for math modeling

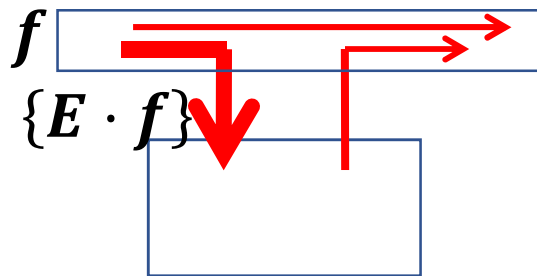
First-pass extraction fraction

$$\frac{dC_i(t)}{dt} = \underbrace{\{E \cdot f\}} \cdot Ca(t) - \underbrace{\{E \cdot f\}} \cdot C_v(t)$$

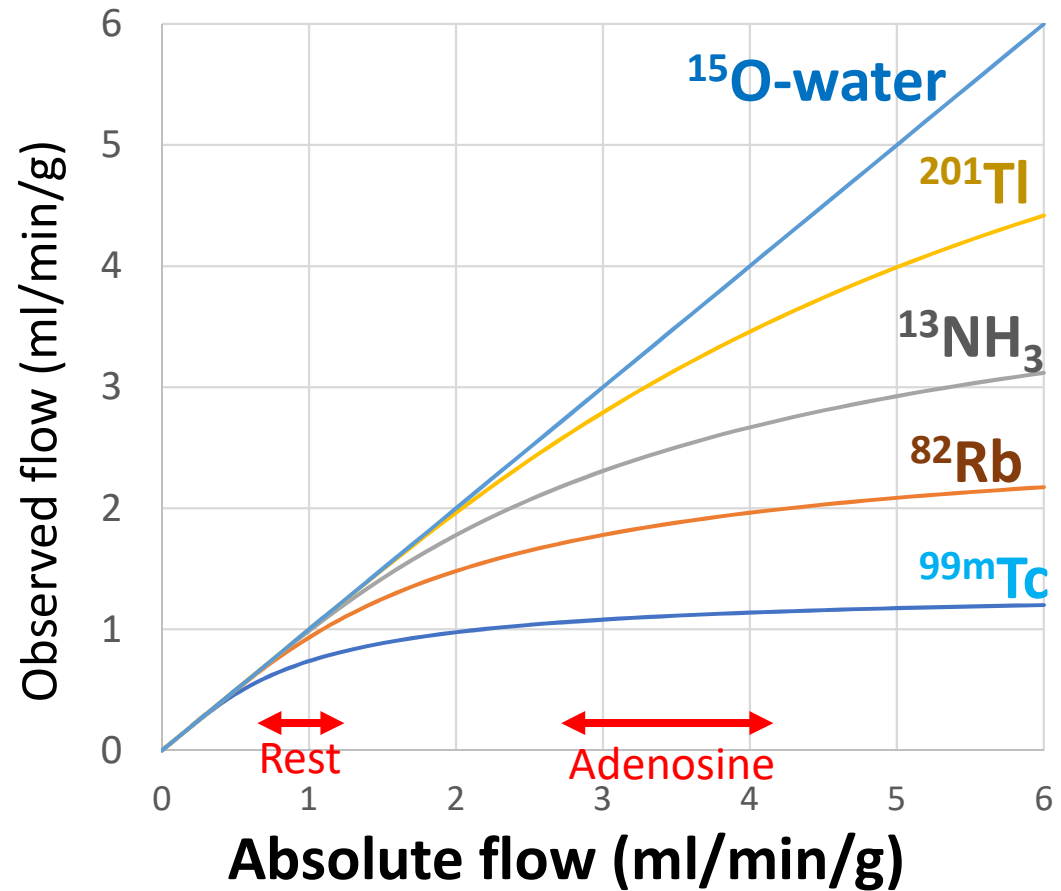
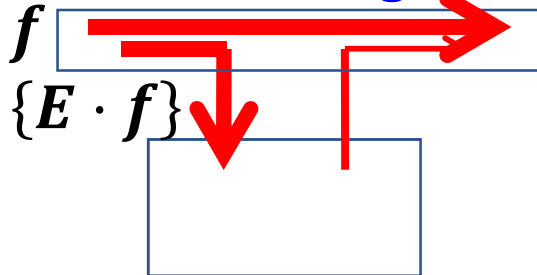
Ideal



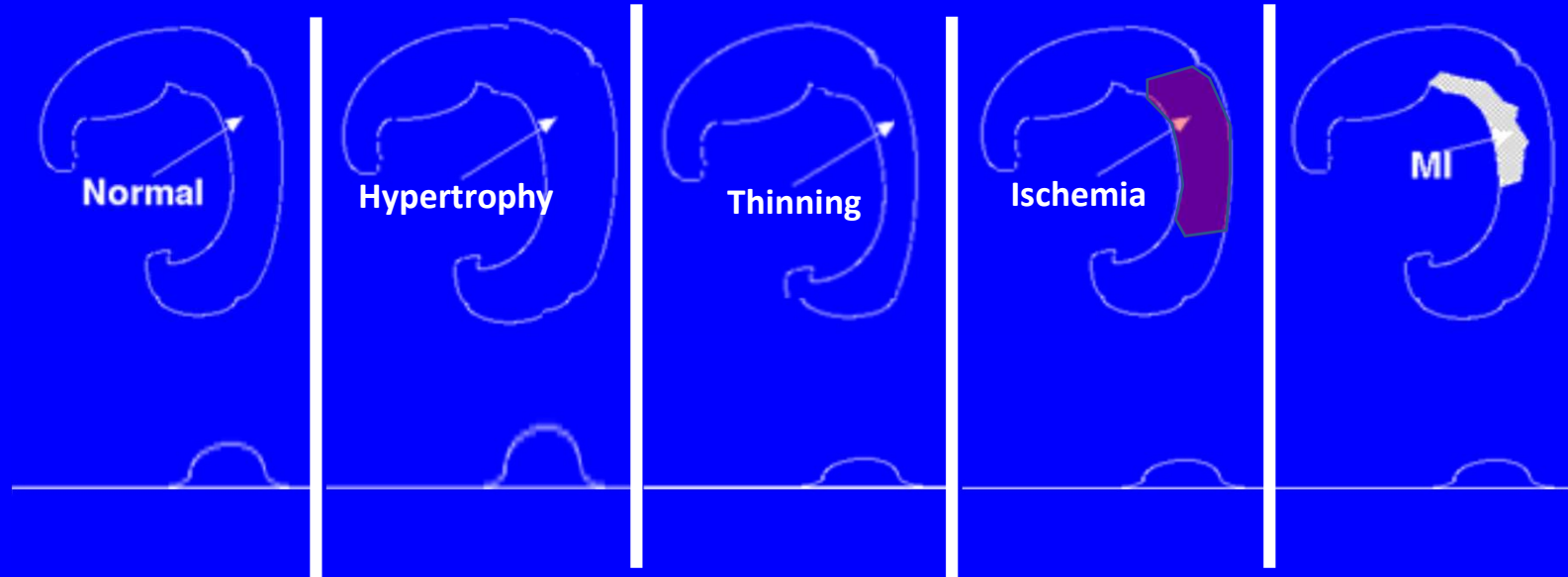
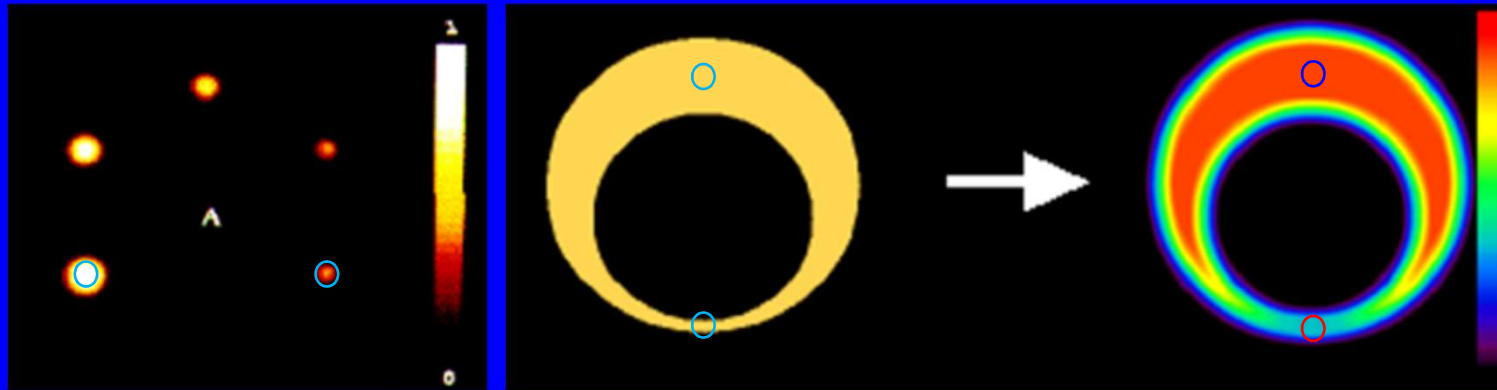
Limited EF at rest



Limited EF during stress



Systematic underestimation due to Partial Volume Effect (PVE) in Myocardial PET



Partial Volume Correction in Myocardial Blood Flow Quantitation



Recovery coeff.

$$\alpha = \frac{M^{tissue}}{V^{ROI}} \left[\frac{g}{ml} \right]$$

Arterial blood
volume

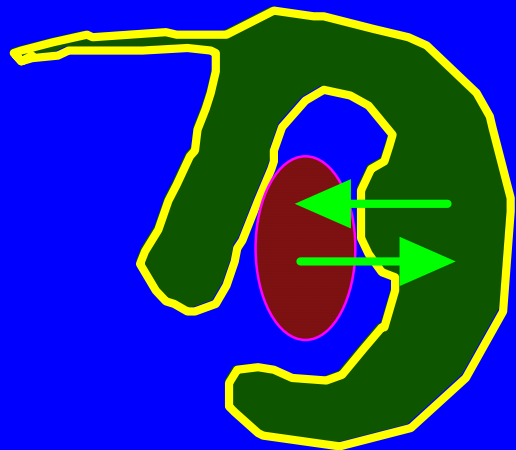
$$R(t) = \alpha f \cdot C_a(t) \otimes e^{-\frac{f}{P}t} + V_a C_a(t)$$

Water Perfusable Tissue Fraction (PTF)

Use of LV TAC and Spillover Correction ¹⁵O-Water Myocardial PET

Fitting f , α and V_a to $R(t)$

Spillover correction

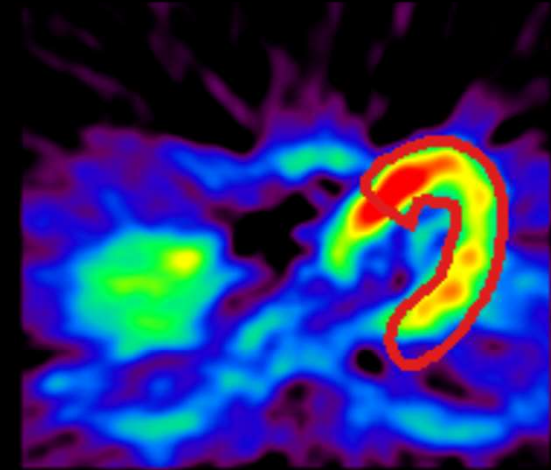
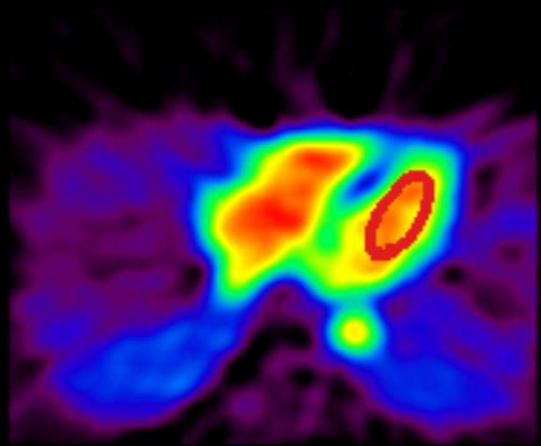
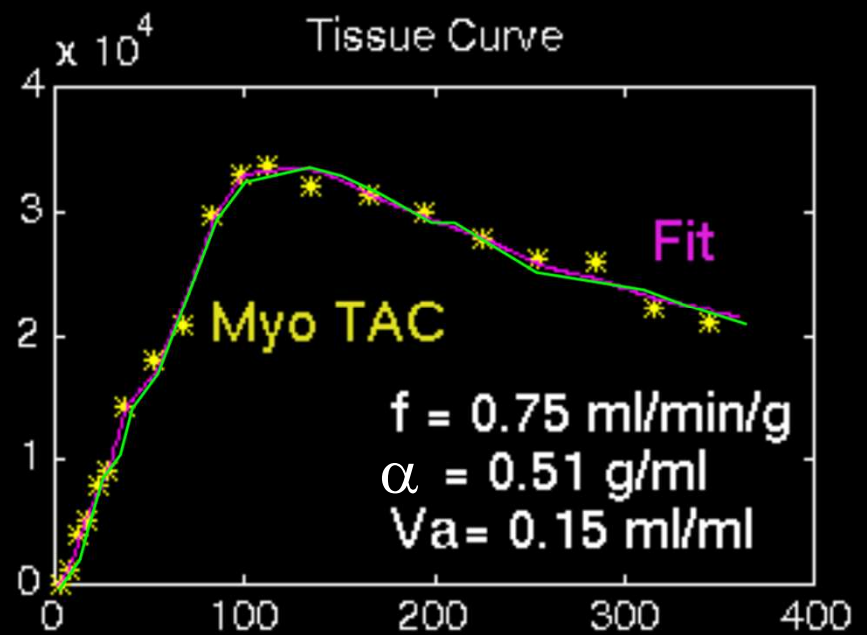
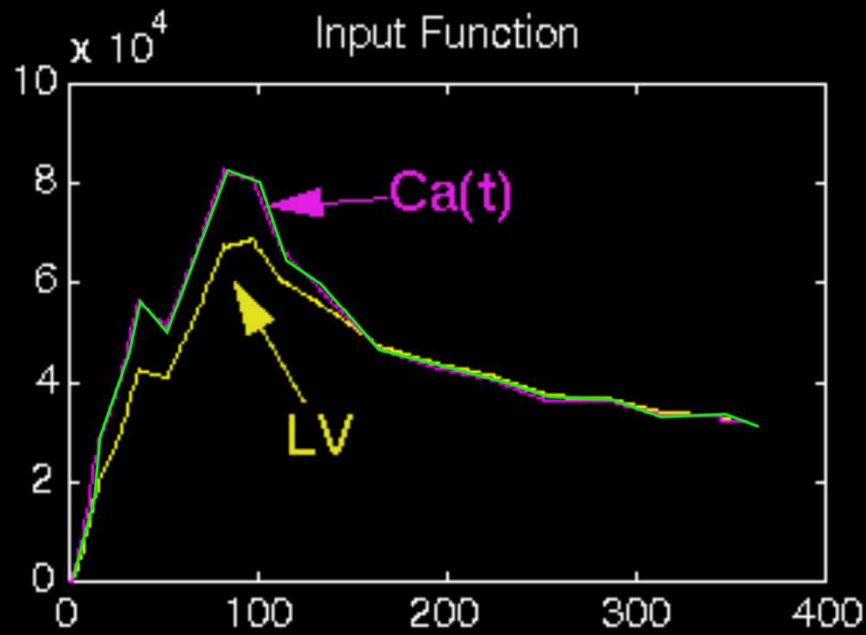


$$R(t) = \alpha C_i(t) + V_a C_a(t)$$

$$LV(t) = \beta C_a(t) + (1-\beta) C_i(t)$$

JNM 1992; 33:1669-1677

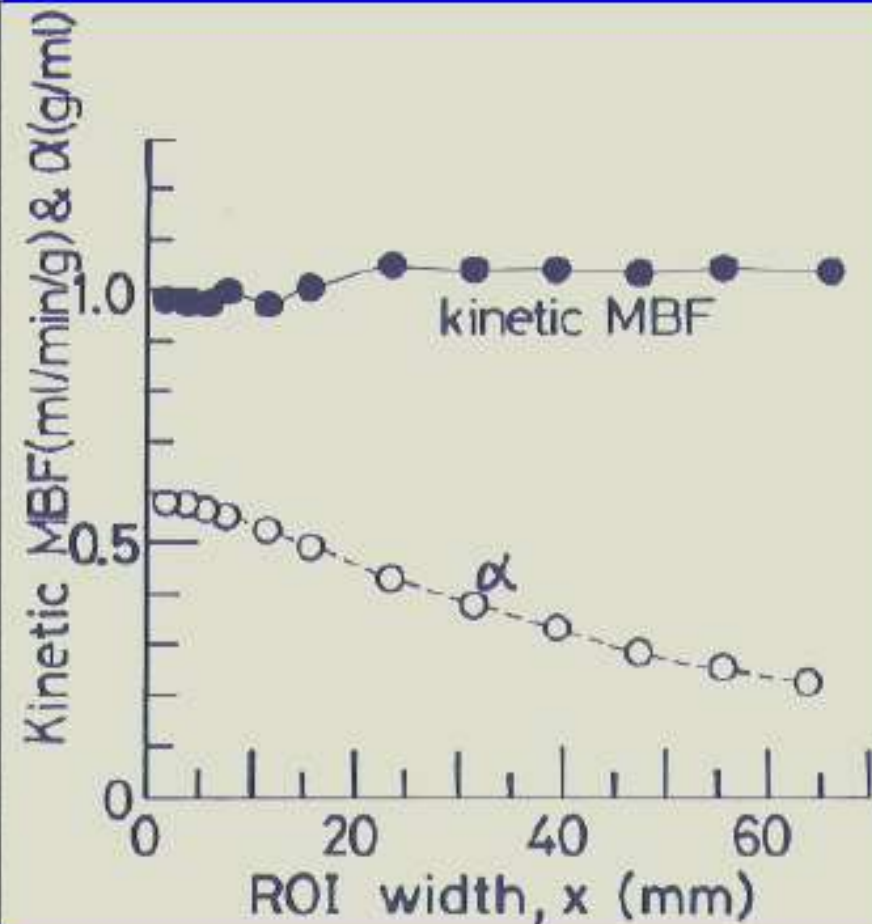
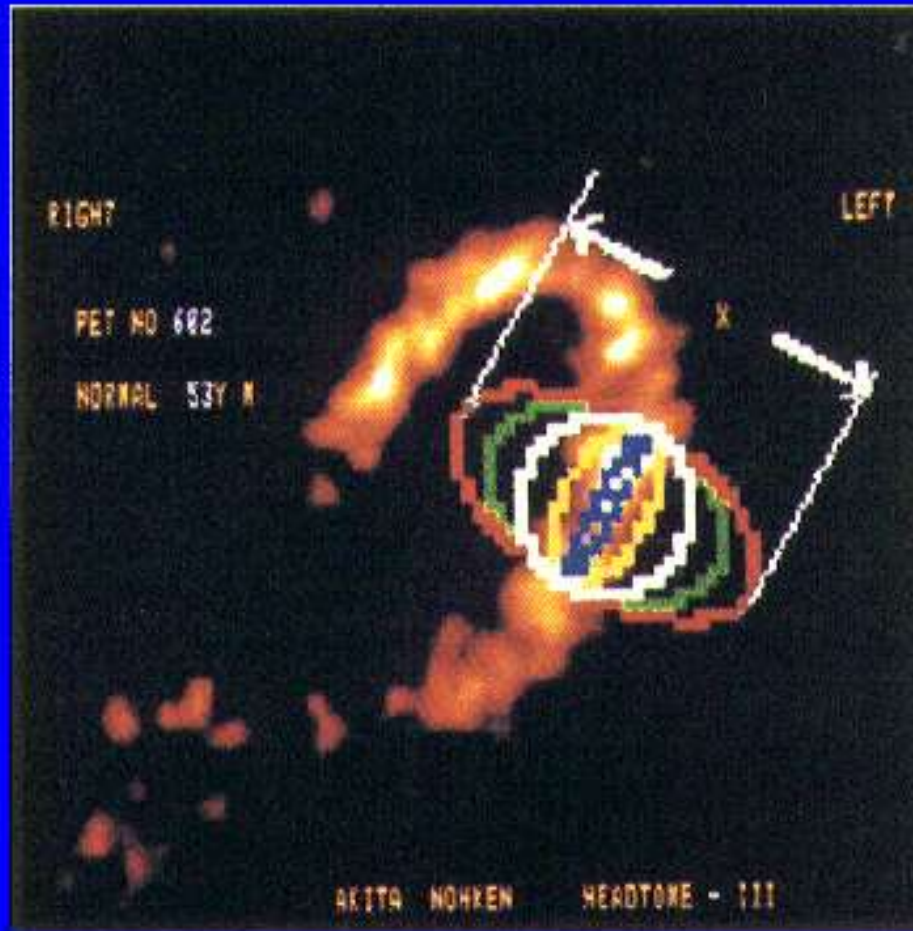
JNM 1995; 36:78-35



Iida et al., J Nucl Med 1992; 33:1669-1677

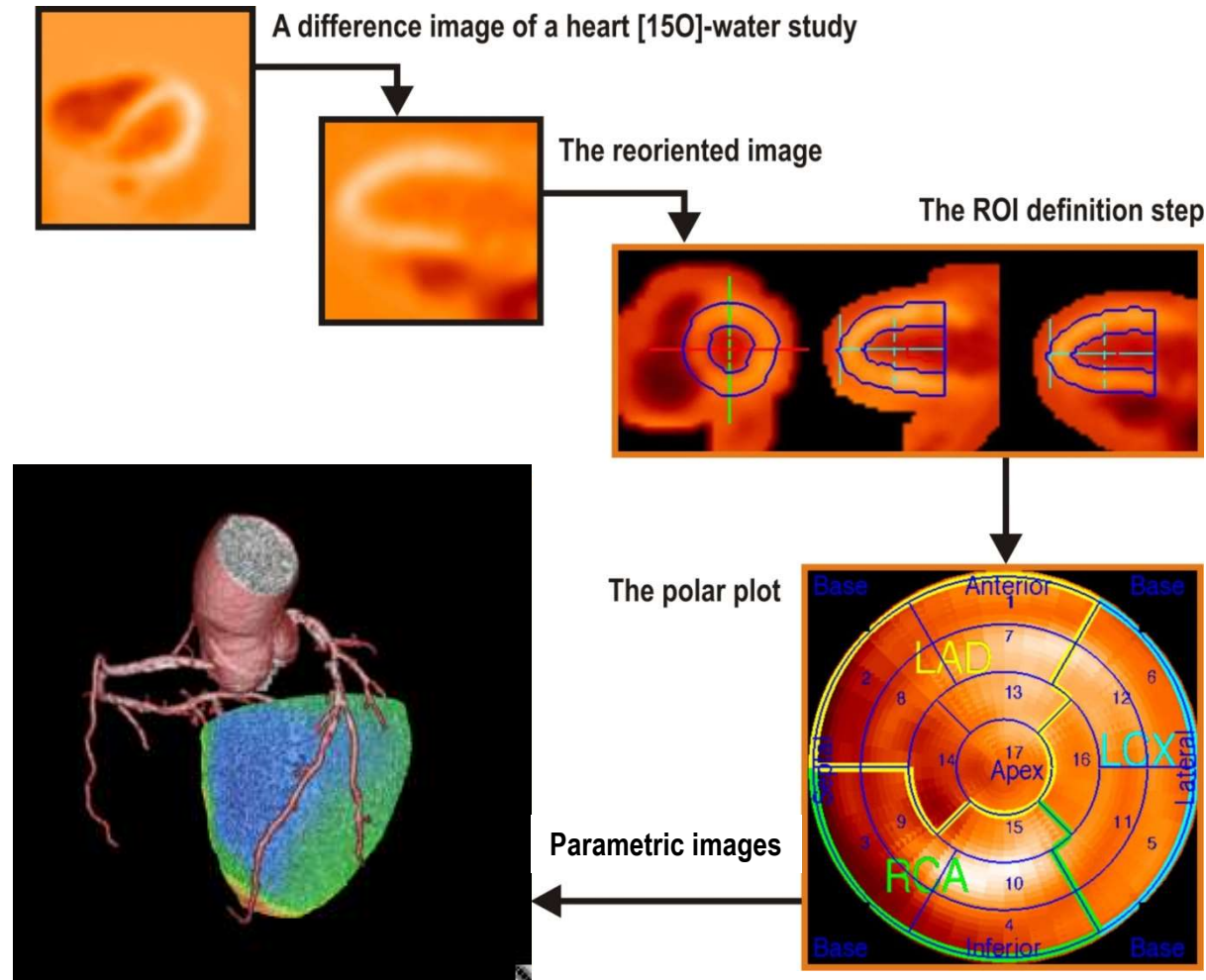
Validation of MBF Quantification by Use of O-15 Water

ROI Size Dependency of Estimated MBF



Iida et al Circulation 1988; 78:104-115

Analysis of PET myocardial perfusion study



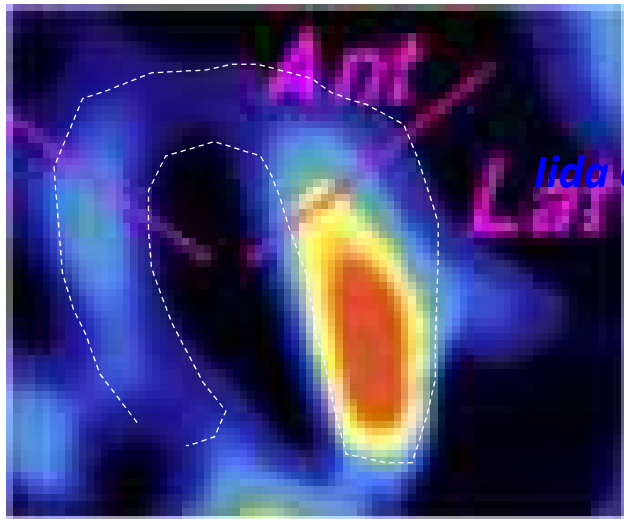
Software packages for MBF quantification:

- aQuant
- Cardiac Vuer
- Munich Heart
- PMOD
- FlowQuant
- Carimas
- Syngo
- Hoquto
- QPET
- UW-QPP
- ImagenQ
- Corridor 4DM

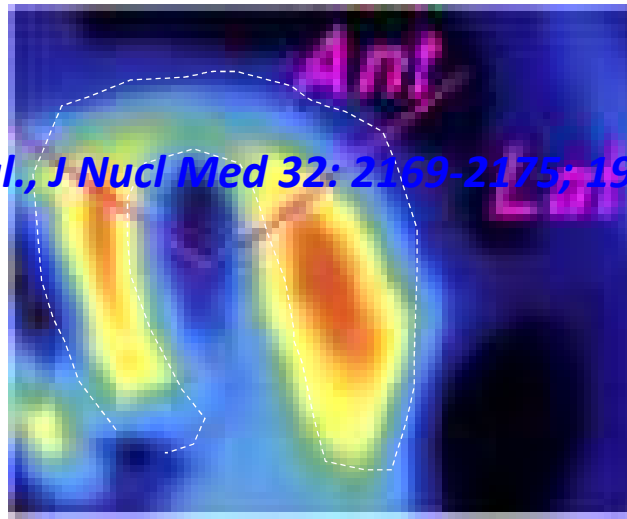
Carimas™ / Turku PET Centre

Courtesy of Prof. J. Knuuti

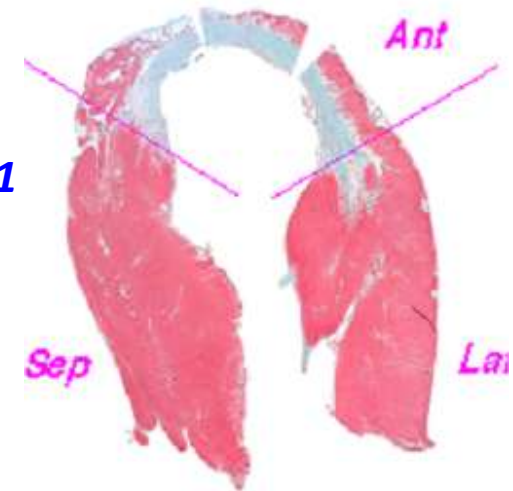
MBF and water-perfusable tissue (PTF) by ^{15}O -water PET in a K9 model of OMI



MBF
(ml/min/mL)



PTF
(g/mL)

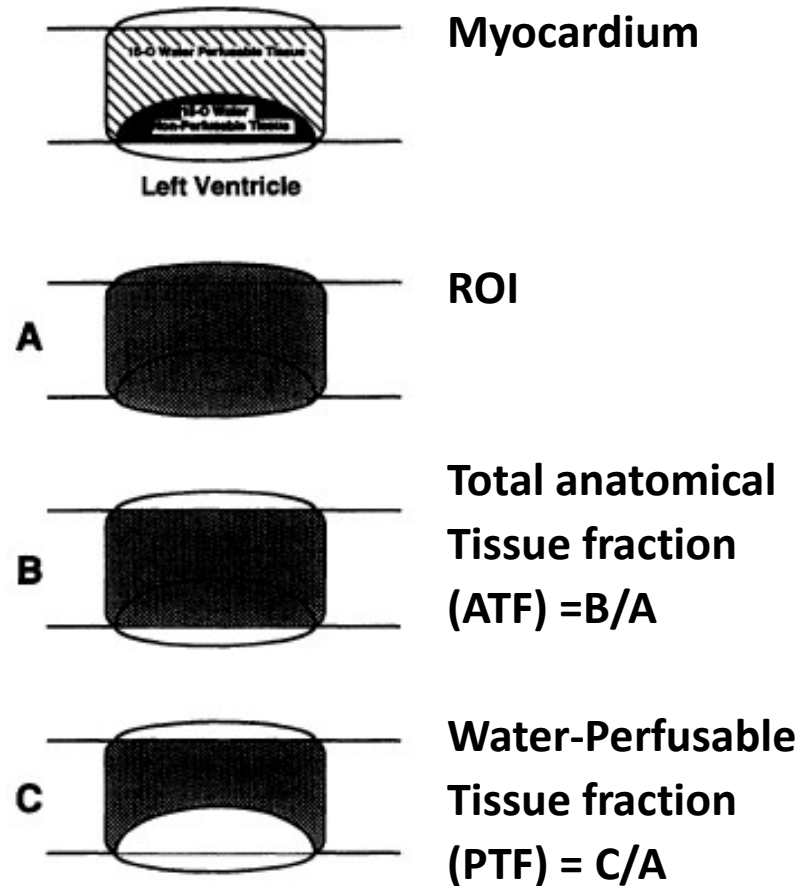


EM

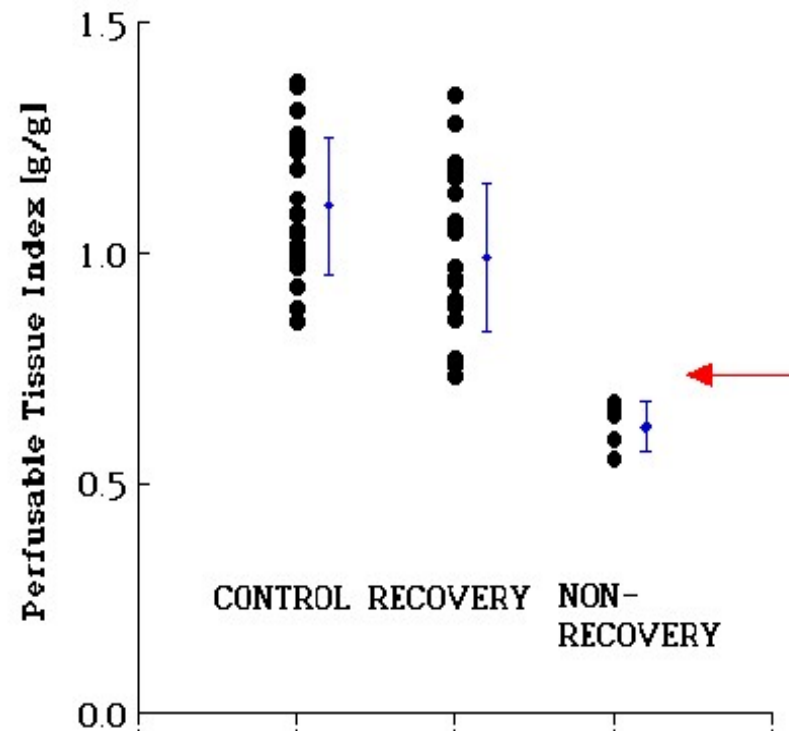
Iida et al., J Nucl Med 32: 2169-2175, 1991

Iida et al J Nucl Med. 41:1737-1745., 2000

PTI as a Myocardial Viability Marker

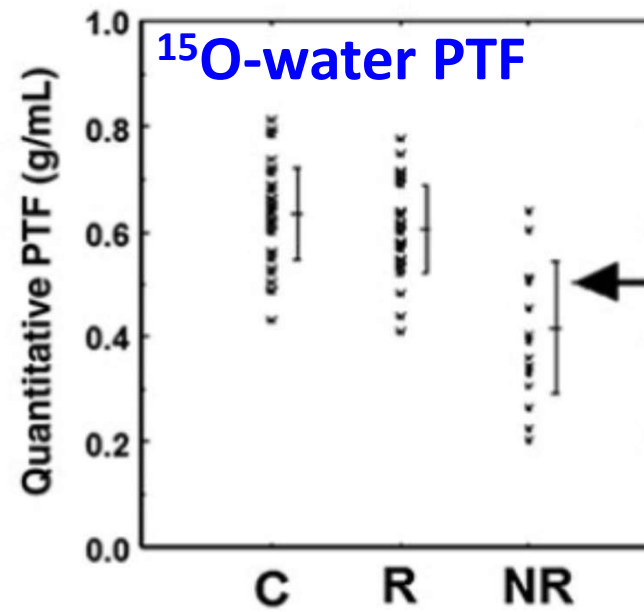
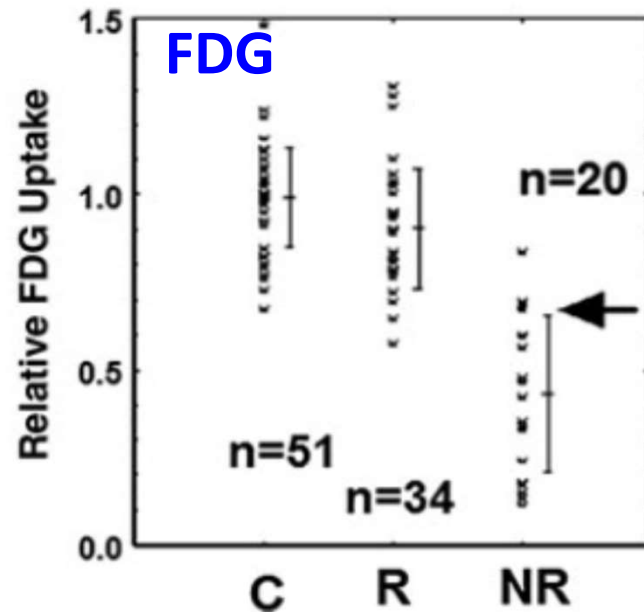


PTI values before CABG

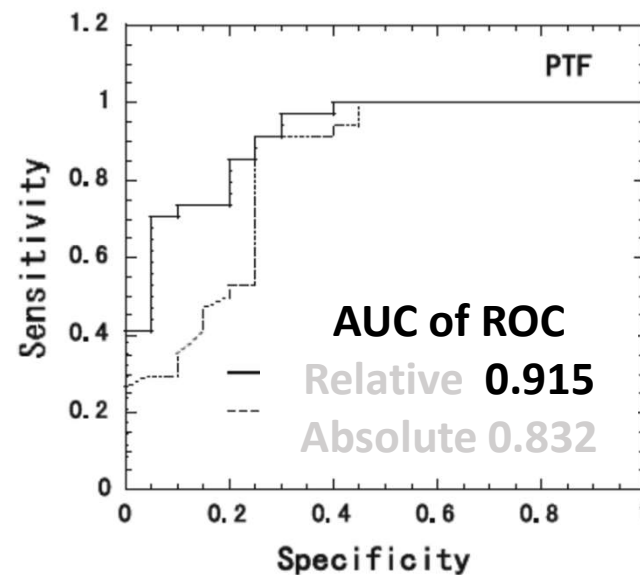
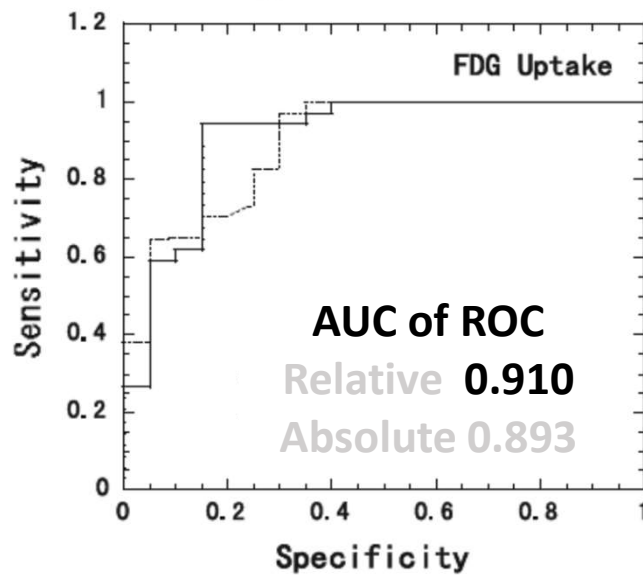


Yamamoto et al, Circulation, 1992
De Silva et al, Circulation, 1993

FDG & PTF as Myocardial Viability Marker



PTF: 70% of normal



16 Patients
128 ROIs

Perfusable Tissue Index as a Potential Marker of Fibrosis in Patients with Idiopathic Dilated Cardiomyopathy

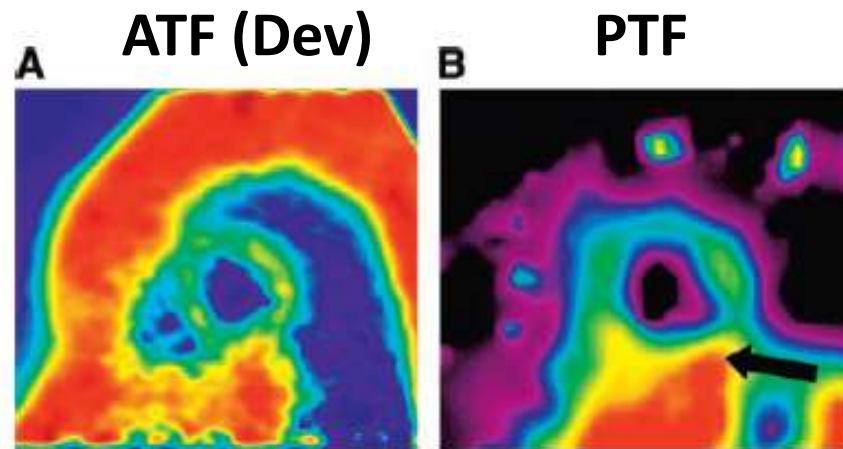


FIGURE 1. Short-axis ATF (A) and PTF (B) images of a healthy volunteer. Arrow in PTF image indicates inferior wall. Spillover effects from adjacent liver tissue are present.

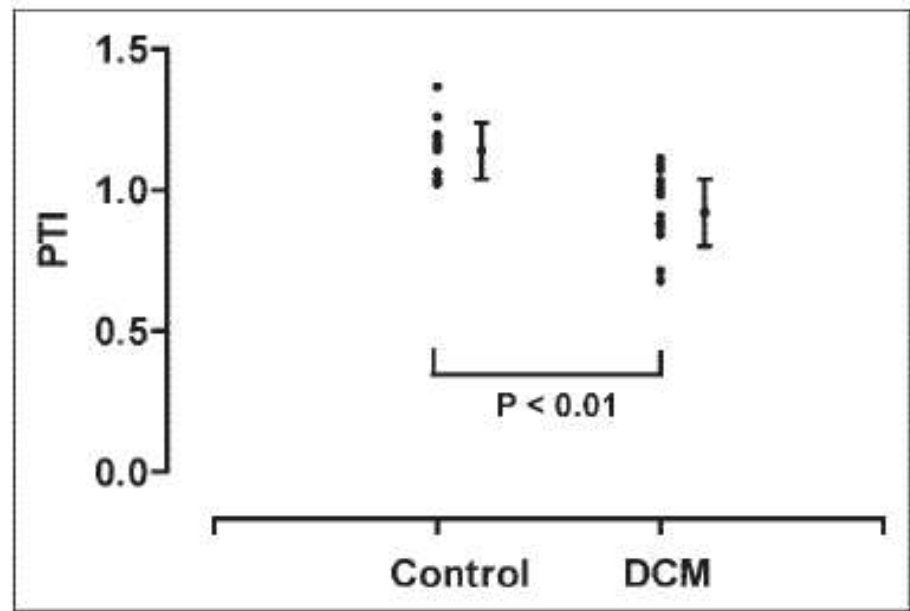


FIGURE 2. PTI for healthy control subjects and DCM patients.

Knaapen P et al., J Nucl Med. 45:1299–1304, 2004

Missing issues in this talk

1. Modeling for metabolic tracers, e.g., ^{18}F -FDG
2. Modeling for neuro-receptor ligands (reversible tracers) and application to drug development and evaluation.
3. Appearance of metabolized molecules in the blood
4. Examples where the existing compartment model is limited or does not work.
5. etc

Future perspectives

Mismatch between PET and CT images in attenuation correction

⇒ A novel approach for attenuation correction is needed

Metabolites in the AIF

⇒ Total body PET to estimate the metabolites in the arterial blood

Logistical complexity that made the usage of ^{15}O -oxygen inhalation PET difficult

⇒ Comprehensive automated radio-tracer production + inhalation system

⇒ Single Scan Dual Administration (SSDA) with sequential $^{15}\text{O}_2$ and H_2^{15}O

CT and PET mismatch

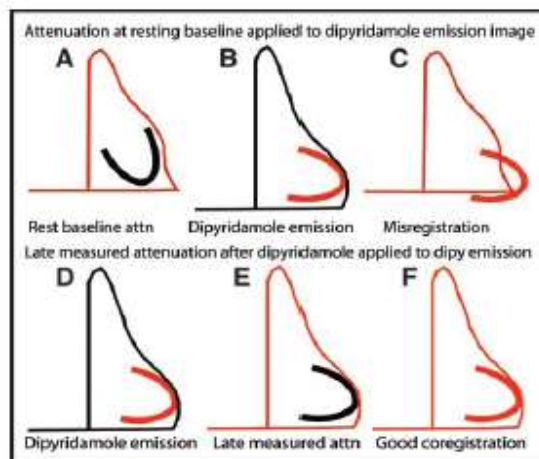
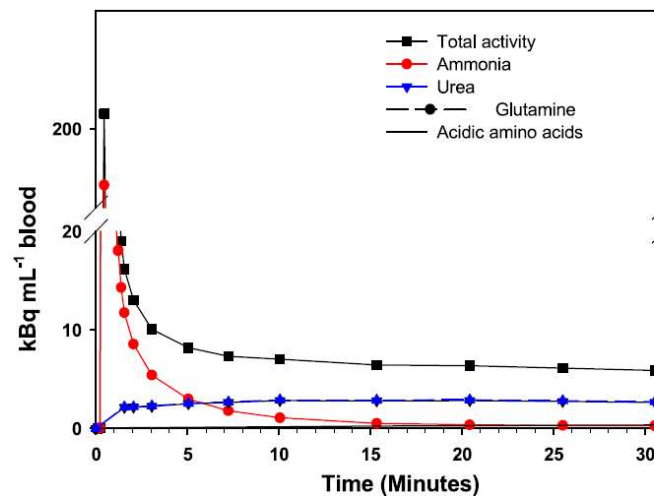
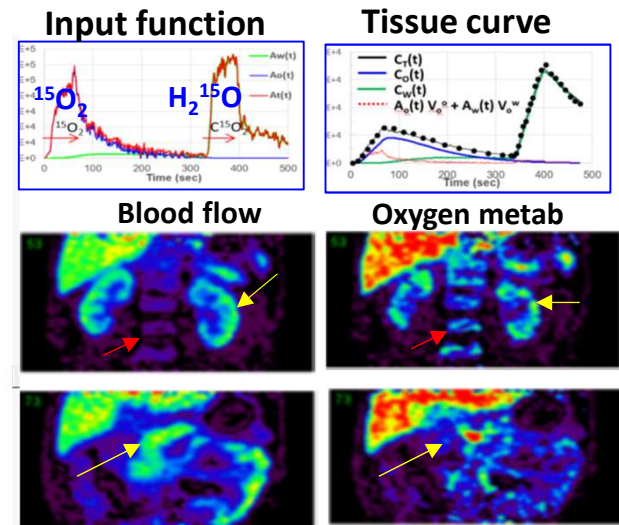


FIGURE 7. Mechanisms for attenuation artifacts using post-dipyridamole scan. Legend is the same as Figure 6.

Metabolites in AIF



SSDA ^{15}O -Gas PET



Total Body PET scanner with axial FOV of 106 cm

Biograph Vision Quadra - Siemens Healthineers

